Broadly-neutralizing antibodies that bind to the influenza hemagglutinin stalk domain enhance the effectiveness of neuraminidase inhibitors via Fc-mediated effector functions

Ali Zhang[1,2,3], Hanu Chaudhari[1,2,3], Yonathan Agung[1,2,3], Michael R. D'Agostino[1,2,3], Jann C. Ang[1,2,3], Matthew S. Miller[1,2,3†]

[1]Michael G. DeGroote Institute for Infectious Diseases Research, McMaster University, Hamilton, ON, Canada, L8S 4K1

[2]McMaster Immunology Research Centre, McMaster University, Hamilton, ON, Canada, L8S 4K1

[3]Department of Biochemistry and Biomedical Sciences, McMaster University, Hamilton, ON, Canada, L8S 4K1

†To Whom Correspondence Should be Addressed

Corresponding author contact: mmiller@mcmaster.ca

Keywords: influenza virus; broadly-neutralizing antibodies; oseltamivir; NA inhibitors; antibodies; Fc receptors; antivirals, antibody-dependent cell cytotoxicity

34

Summary (117/150 words)

36

The conserved hemagglutinin stalk domain is an attractive target for broadly effective antibody-based therapeutics and next generation universal influenza vaccines. Protection provided by hemagglutinin stalk binding antibodies is principally mediated through activation of immune effector cells. Titers of stalk-binding antibodies are highly variable on an individual level, and tend to increase with age as a result of increasing exposures to influenza virus. In our study, we show that stalk-binding antibodies cooperate with neuraminidase inhibitors to protect against influenza virus infection in an Fc-dependent manner. These data suggest that the effectiveness of neuraminidase inhibitors is likely influenced by an individual's titers of stalk-binding antibodies, and that neuraminidase inhibitors may enhance the effectiveness of future stalk-binding monoclonal antibody-based treatments.

46

Introduction

48

Influenza causes 3-5 million serious illnesses and 290,000 – 645,000 deaths every year worldwide (Iuliano et al., 2018). Seasonal influenza vaccination induces production of mostly neutralizing antibodies directed against the hemagglutinin (HA) head domain and is the most effective way to prevent infection. The HA head domain undergoes continuous antigenic drift, which necessitates annual reformulation of seasonal vaccines to narrow strain-specific protection. Novel vaccine strategies designed to elicit immune responses against more conserved protein domains, such as the HA stalk domain by broadly neutralizing antibodies (bNAbs), may achieve more broad and durable protection against influenza.

56

The HA stalk domain is more conserved between influenza virus strains compared to the HA head domain due to functional constraints and minimal immune pressure (Kirkpatrick et al., 2018; Wu and Wilson, 2017). Protection against influenza by HA stalk-binding antibodies is mediated primarily by Fc-dependent activation of immune effector cells (DiLillo et al., 2016, 2014; He et al., 2016). Optimal Fc activation by these antibodies requires two points of contact: the antibody Fab-HA stalk interaction, and the sialic acid-HA head interaction (Leon et al., 2016) (Figure 1A). Neuraminidase (NA), the other major influenza virus surface glycoprotein, cleaves sialic acids from the HA head domain during viral budding. Antibody dependent cellular cytotoxicity (ADCC) is a process through which infected cells are eliminated by Fc receptor (FcR)-bearing immune cells after binding of antibodies to surface-bound antigen. Antibodies that bind to NA can induce modest levels of ADCC on their own and can also cooperate with stalk-binding antibodies to enhance ADCC induction (He et al., 2016). HA-stalk binding antibodies can, in turn, partially inhibit neuraminidase activity, contributing to

68 their potency of virus neutralization (Kosik et al., 2019). Since cleavage of the sialic acid-HA head interaction

69 by neuraminidase may destabilize one of the two points of contact required for optimal stalk antibody-mediated

70 activation of immune effector cells, we reasoned that chemical inhibition of NA activity may also potentiate

71 ADCC induction by HA stalk-binding antibodies.

72

73 Here, we show that chemical inhibition of neuraminidase increases stalk antibody Fc-mediated activation of

74 immune effector cells in a dose dependent manner. HA stalk antibodies potentiated the efficacy of the NA

75 inhibitor oseltamivir in both prophylactic and therapeutic contexts. This effect is preserved in the contexts of

76 both monoclonal stalk antibody and polyclonal sera. Cooperativity between neuraminidase inhibition and HA

77 stalk antibodies was dependent on Fc-FcR interaction. Together, these data suggest that the efficacy of

78 oseltamivir treatment may be dependent on HA stalk antibody titers, and that monoclonal HA stalk antibodies

79 and neuraminidase inhibitors may represent an effective combination therapy in the future.

80

81 **Results**

82

83 **Oseltamivir cooperates with stalk-binding antibodies to enhance antibody-dependent cell**

84 **cytotoxicity of cells infected with group 1 and group 2 influenza A viruses.**

85

86 We first set out to determine the role of neuraminidase on HA stalk-binding antibody mediated activation of

87 immune effector cells. We first quantified the NA activity of three representative strains of influenza virus,

88 A/Puerto Rico/8/1934 H1N1 (PR8), A/California/07/2009 H1N1 (Cal/09), and X-31 H3N2 (Figures S1A-S1C)

89 (Kilbourne, 1969). We then tested the potency of oseltamivir in inhibiting the NA activity of these strains

90 (Figures S1D-F), and in reducing viral replication (Figures S1G-S1I). Having established these dose-response

91 relationships with oseltamivir, we performed antibody dependent cell cytotoxicity (ADCC) assays using

92 modified Jurkat effector cells expressing murine FcγRIV. This is an extremely sensitive, highly quantitative

93 assay that we have used extensively in the past and has been validated to correlate closely with the activation of

94 primary NK cells (Chromikova et al., 2020; He et al., 2016). A549 target cells were infected with PR8, Cal/09,

95 or X-31 at an MOI of 5. The infected cells were then incubated with oseltamivir and murine monoclonal stalk-

96 binding broadly neutralizing antibodies (bNAbs) 6F12 for cells infected with PR8 and Cal/09 (which express

97 group 1 HA), and 9H10 for cells infected with X-31 (which expresses group 2 HA). Infection and binding

98 specificity of antibodies was verified by immunofluorescence microscopy (Figure S2). Addition of oseltamivir

99 resulted in a dose-dependent enhancement of ADCC induction in PR8, Cal/09 and X-31 infected cells (Figures

100 1B-D). Enhancement of bNAb-mediated ADCC by oseltamivir required Fc-FcR interaction, as 6F12 with the

101 D265A mutation, which abrogates FcR binding, failed to induce ADCC of PR8 infected cells, even at the

102 highest oseltamivir concentration used (Figure 1E). Together, these results demonstrate that NA inhibition by

103 oseltamivir enhances ADCC induction by bNAbs that bind to the HA stalk domain, demonstrating cooperative

104 activation.

105

106 **The efficacy of oseltamivir in preventing and treating influenza virus is potentiated by bNAbs**

107

108 To determine whether bNAbs could enhance protection mediated by oseltamivir *in vivo*, we conducted

109 influenza challenge experiments in a murine model system. To test efficacy in a prophylaxis setting, six groups

110 of 6-8 week old BALB/c mice (n = 5 mice/group) were administered 1mg/kg 6F12, 6F12 D265A, or IgG

111 isotype control intraperitoneally and 1mg/kg oseltamivir or PBS by oral gavage. The mice were then infected

112 with $5 \times LD_{50}$ of PR8 (500 plaque-forming units (PFU)) intranasally two hours later. Mice continued to receive

113 either oseltamivir or PBS twice daily by oral gavage for 5 days and were monitored for 14 days, with the

114 humane endpoint defined as 80 % of initial body weight (Figures 2A-C). Mice that received negative control

115 treatments all reached endpoint by day 7 post-infection. Of the mice that did not receive oseltamivir, treatment

116 with 1 mg/kg 6F12 resulted in similar disease progression compared to the IgG isotype control. Similarly, mice

117 that received oseltamivir alone experienced significant weight loss. In contrast, mice that received both

118 oseltamivir and 6F12 lost minimal weight throughout the experimental period, with none reaching endpoint.

119 Mice that received both oseltamivir and 6F12 D265A displayed similar disease progression compared to mice

120 that received oseltamivir alone, demonstrating that Fc-FcR interactions are crucial for the enhanced protection

121 offered by co-administration of 6F12 and oseltamivir.

122

123 To determine if bNAbs could also enhance the activity of oseltamivir when treating an established influenza

124 infection, we infected four groups of 6-8 week old BALB/c mice (n = 5 mice/group) with $5 \times LD_{50}$ of PR8 (500

125 PFU) and treated with 10mg/kg 6F12 or 10mg/kg oseltamivir starting 2 days post-infection (Figures 2D-E).

126 Antibody or oseltamivir alone were insufficient to protect mice from severe disease, whereas the combination of

127 6F12 and oseltamivir yielded complete protection. These results demonstrate a substantial improvement in

128 protection against influenza morbidity and mortality when oseltamivir and stalk-binding antibodies are

129 administered together in the context of both prophylaxis and treatment. The cooperativity of oseltamivir and

130 stalk-binding antibodies was not due to their independent activities (i.e., direct neuraminidase inhibition and

131 virus neutralization), but was instead dependent upon Fc-FcR interactions mediated by the stalk-binding

132 antibodies.

133

134 **Titers of bNAbs in human serum predict effectiveness of oseltamivir treatment**

135

136   The previous results demonstrate that oseltamivir cooperates with monoclonal stalk-binding antibodies to

137   protect against clinical signs of influenza virus infections by enhancing antibody Fc-mediated immune effector

138   cell activation. We next set out to determine if titers of bNAbs in human serum could predict the effectiveness

139   of oseltamivir treatment. First, we conducted ADCC assays using serum from 4 adult donors who had received

140   the seasonal influenza vaccine 14 days prior to serum collection. Titers of bNAbs in these samples were first

141   quantified by ELISA using a chimeric cH6/1 hemagglutinin protein, that contains the head domain from

142   A/Mallard/Sweden/81/02 H6N1 and the stalk domain from A/Puerto Rico/8/1934 H1N1 (Figures 3A and 3B).

143   The cH6/1 chimera has been used extensively in the past to quantify antibodies that specifically bind to the

144   group 1 stalk domain, as humans are rarely exposed to H6 influenza viruses and we have previously shown that

145   human sera lacks hemagglutination inhibition (HAI) activity against the H6 head domain (Miller et al., 2013b;

146   Nachbagauer et al., 2014; Pica et al., 2012; Sangster et al., 2013). Consistent with the observations made using

147   monoclonal bNAbs, ADCC induction by polyclonal bNAbs from human donors was enhanced by oseltamivir

148   (Figures 3C-3F).

149

150   We next set out to assess the effectiveness of human sera in combination with oseltamivir in protecting against a

151   representative "pandemic-like" virus. We then chose to use A/Vietnam/1203/2004 H5N1 HAlo (Viet/04), which

152   is a an H5N1 virus that is highly pathogenic in mice, but has had the polybasic cleavage site of the H5 protein

153   removed to enhance safety (Steel et al., 2009). ELISAs were first performed on the serum from two additional

154   healthy adult donors using the chimeric cH6/1 hemagglutinin protein to quantify bNAb titers (Figures S3A and

155   S3B)., To ensure that the serum samples used in these assays did not contain HAI+ antibodies to the head

156   domain of Viet/04 H5, we conducted a HAI assay (Figure S3C). No HA inhibition was observed, indicating that

157   both donors were naïve to this virus. In ADCC assays, the donor with higher titers of HA stalk-binding

158   antibodies based on ELISA data (Figure S3A) also elicited higher activation of reporter cells, consistent with

159   expectations (Figure S3D).

160

161   Next, six groups of 6-8 week old BALB/c mice were either administered 150ul of serum with low titers of stalk-

162   binding antibodies (Low Serum), 150ul of serum with high titers of stalk-binding antibodies (High Serum), or

163   150ul of PBS (vehicle). The mice were also given either 0.1mg/kg oseltamivir or PBS by oral gavage. The mice

164   were infected with $5 \times LD_{50}$ of Viet/04 H1N1 (200 PFU) intranasally two hours after passive transfer of serum

165   (Figure 4A). The data is displayed as two sets of graphs for clarity, with shared negative control groups (Figures

166   4B-4E). Mice that received either serum or oseltamivir alone experienced significant morbidity, with most

167   animals in those groups reaching endpoint. When oseltamivir was administered to mice that had received serum

168   containing low titers of bNAbs (Low Serum), weight loss was similar to that of mice treated with serum or

169   oseltamivir alone; however, mortality in this group improved substantially, with only 1 out of 5 mice reaching

170   endpoint. In contrast, when oseltamivir was administered to mice that received serum containing high titers of

171 bNAbs (High Serum) minimal weight loss was observed, and full protection against mortality was achieved

172 (Figures 4B-4E). Taken together, these results demonstrate that titers of bNAbs found in human serum can

173 significantly impact the efficacy of oseltamivir treatment.

174

175 **Discussion**

176

177 Neuraminidase inhibitors are a major class of antivirals used for treatment and prevention of influenza virus.

178 While NA inhibitors tend to be highly effective in preventing influenza when administered prophylactically,

179 effectiveness is much more modest in most therapeutic contexts (Doll et al., 2017). Maximum benefit is

180 achieved therapeutically when NA inhibitors are administered early after symptom onset (Fry et al., 2014; Hiba

181 et al., 2011; Rodríguez et al., 2011). However, there is considerable heterogeneity in the effectiveness of these

182 drugs at the individual level, and the host factors that determine outcome remain elusive (Jefferson et al., 2014).

183 Furthermore, neuraminidase inhibitor-resistant viruses circulate naturally, and therefore strategies that mitigate

184 the selection of these resistant variants are critical to prolonging the utility of this class of drug (Lampejo,

185 2020).

186

187 The hemagglutinin stalk domain is an attractive target for antibody-based therapeutics and universal influenza

188 vaccines due to its high degree of conservation amongst diverse influenza viruses. The main mechanism by

189 which these antibodies protect against influenza is through Fc-dependent effector cell functions, such as ADCC,

190 NETosis, phagocytosis, and secretion of cytokines (DiLillo et al., 2016, 2014; He et al., 2017; Stacey et al.,

191 2021). Elegant studies by the Yewdell laboratory previously demonstrated that NA inhibition by anti-HA stalk

192 antibodies contributes to viral neutralization and induction of FcγR-mediated activation of innate immune cells

193 (Kosik et al., 2019). We have also previously shown that antibodies with NAI activity can cooperate with

194 bNAbs that bind to the HA stalk to potentiate ADCC (He et al., 2016). Our current study demonstrates that the

195 efficacy of NA inhibitors is profoundly influenced by pre-existing titers of bNAbs, and that protection from

196 influenza *in vivo* is mediated by potentiation of Fc-dependent effector functions of immune cells mediated by

197 NA inhibition.

198

199 We used the well-characterized monoclonal murine antibodies 6F12 and 9H10, which bind to H1 and group 2

200 HA respectively, in our ADCC assays (Tan et al., 2014, 2012). Our ADCC assay uses engineered Jurkat

201 effector cells, which express murine FcγRIV and firefly luciferase driven by the nuclear factor of activated T

202 cells (NFAT) response element. ADCC induction in these assays correlate well with classical CD107a NK cell

203 degranulation assays (Chromikova et al., 2020). We found that oseltamivir potentiated ADCC induced by

204 bNAbs in a dose-dependent manner. Intact Fc-FcR interactions were absolutely necessary for this potentiation,

205 as introduction of a D265A mutation in the CH2 domain of 6F12, which abolishes the Fc-FcR interaction,

206 negated effector cell induction (Baudino et al., 2008; Nimmerjahn et al., 2005; Temming et al., 2020). The

207 addition of oseltamivir had similar effects in improving ADCC mediated by serum from healthy donors.

208 Effector cell activation is strikingly enhanced even in samples with low titers of bNAbs. Antibodies targeting

209 the less immunogenic NA, M2, and NP have also been shown to induce effector cell activation (DiLillo et al.,

210 2016; Jegaskanda et al., 2017; Lee et al., 2014; Stadlbauer et al., 2019). Our experiments here show that

211 chemical inhibition of neuraminidase can further enhance induction of ADCC even in a complex, polyclonal

212 context.

213

214 Consistent with previous studies, we found that co-administration of oseltamivir with a sub-protective dose of

215 monoclonal HA stalk-binding antibodies improve protection against lethal influenza challenge in mouse models

216 (Nakamura et al., 2013; Paules et al., 2017). However, our work clearly demonstrates that this enhancement is

217 dependent upon Fc-FcR interactions, and is not due to the combined, independent activities of oseltamivir and

218 bNAbs. To test whether titers of bNAbs in human serum might impact the effectiveness of oseltamivir

219 treatment, we passively transferred mice with human sera containing either "low" or "high" titers of bNAbs.

220 The effectiveness of oseltamivir treatment was proportional to the titers of bNAbs transferred to the mice.

221 Together, these data strongly suggest that and individual's pre-existing titers of bNAbs may have a profound

222 impact on the effectiveness of oseltamivir treatment.

223

224 Our data provide new insights that help to explain the heterogeneity in effectiveness of NA inhibitors at the

225 individual level. In the future, human clinical trials that directly assess whether pre-existing titers of bNAbs

226 predict the effectiveness of NA inhibitor treatment could have important clinical implications that inform

227 selection of the most appropriate antiviral treatments for individuals with influenza – especially in light of the

228 recent approval of baloxivir marboxil, which targets the cap-snatching endonuclease activity of the viral

229 polymerase complex (Noshi et al., 2018). These drugs have similar clinical effectiveness and thus, an evidence-

230 based framework to guide which drug may be most effective for individual patients is sorely needed. While

231 rapid screening of bNAb titers may be possible in the future, it is also known that titers of these antibodies tend

232 to increase with age (Miller et al., 2013a; Nachbagauer et al., 2016). Our study also suggests that the

233 effectiveness of future bNAb-based monoclonal antibody therapies could be improved by coadministration with

234 NA inhibitors. This class of drugs may be especially important for providing first-line defense in the event of a

235 future influenza virus pandemic, since prediction of which strains are likely to cause pandemics remains a

236 considerable challenge to strain-specific pandemic vaccine design (Miller and Palese, 2014).

237

241   M.S.M was also supported, in part, by a CIHR Early Investigator Award and an Ontario Early Researcher

242   Award. M.S.M. holds a Canada Research Chair in Viral Pandemics. A.Z is supported by a Physician Services

243   Incorporated Research Trainee Fellowship and a CHIR Canada Graduate Scholarships – Doctoral Award.

244   M.G.D. was supported, in part, by an Ontario Graduate Scholarship.

245

246   **Author Contributions (29 words)**

247   Conceptualization, A.Z. and M.S.M.; Methodology, A.Z. and M.S.M.; Formal Analysis, A.Z., H.C., Y.A.,

248   J.C.A., and M.S.M; Investigation, A.Z., H.C., Y.A., M.R.D., and J.C.A.; Writing, A.Z. and M.S.M.;

249   Supervision, M.S.M

250

251   **Declaration of Interest (8 words)**

252   The authors have no relevant conflicts of interest.

253

254   **Figure Legends (1160 words)**

255

256   **Figure 1** Oseltamivir potentiates ADCC induction by monoclonal stalk-binding broadly-neutralizing antibodies

257   in a dose-dependent manner.

258

259   (A) Diagram of bNAb facilitating the interaction between immune effector cell and infected cell via two points

260   of contact. The immune effector cell with an Fc receptor is depicted in green. The stalk-binding antibody is

261   shown in grey and blue. The stalk-binding antibody interacts with the HA stalk domain via its Fab portion (1)

262   and binds to the Fc receptor of the effector via its Fc portion. The HA head domain interacts with sialic acid

263   residues on the effector cell (2). NA enzymatically cleaves sialic acids from the HA head domain, abrogating

264   the second point of contact. NA inhibitors, such as oseltamivir, restore the second point of contact by preventing

265   the enzymatic cleavage of HA and sialic acid.

266

267   (B-E) In vitro ADCC assays were completed using A549 cells infected with PR8 (H1N1), Cal/09 (H1N1) or X-

268   31 (H3N2) at an MOI of 5. Fold induction depicts activation above background (infected cells without

269   antibody). Concentrations of oseltamivir carboxylate are denoted in the legend. 6F12 (Pan H1 stalk-binding

270   antibody) was used to target PR8 and Cal/09 infected cells, while 9H10 (Group 2 HA stalk-binding antibody)

271   was used to target X-31 infected cells. Fold induction data is shown as mean ± SD with biological triplicates.

272

273   **Figure 2** Oseltamivir administered in combination with bNAbs is superior at preventing and treating influenza

274   clinical signs compared to either therapeutic alone.

275

276   (A) 6-8 week old female BALB/c mice were infected intranasally with 500 PFU of PR8 ($5 \times LD_{50}$). The mice

277   were also administered intraperitoneally with 6F12 or PBS and an oral gavage of oseltamivir or PBS. A dose of

278   either 1mg/kg 6F12 and/or 1mg/kg oseltamivir (prophylaxis) or 10mg/kg 6F12 and/or 10mg/kg oseltamivir

279   (treatment) were used. The first round of therapeutics was given either 2 hours before infection (prophylaxis) or

280   48 hours after infection (treatment). Mice were then given oseltamivir or PBS by oral gavage twice daily for 5

281   additional days following the first round of therapeutics. Weight change was monitored daily, and the animals

282   were sacrificed when they reached 80% of initial weight.

283

284   (B-C) Weight loss and Kaplan-Meier survival curves of the mice treated prior to infection (prophylaxis group).

285   Weight loss is shown as percent of initial weight with mean ± SEM, n=5/group. Statistical comparisons are

286   shown against the control IgG + PBS group; *p<0.05, **p<0.01. Numbers in brackets denote number of

287   surviving mice and total number of mice per group.

288

289   (D-E) Weight loss and Kaplan-Meier survival curve of the mice treated after infection (treatment group).

290   Weight loss is shown as percent of initial weight with mean ± SEM, n=5/group. Statistical comparisons are

291   against the control IgG + PBS group; *p<0.05, **p<0.01. Numbers in brackets denote number of surviving

292   mice and total number of mice per group.

293

294   **Figure 3** Oseltamivir increases the potency of ADCC induction by polyclonal stalk-binding antibodies.

295

296   (A-B) ELISAs were performed using recombinant cH6/1 HA to measure the titer of H1 stalk-binding antibodies

297   in the serum samples. Absorbance data is shown as mean ± SD. The area under the curve is also shown as mean

298   ± SEM.

299

300   (C-F) In vitro ADCC assays were completed using A549 cells infected with Viet/04 (H5N1) at an MOI of 5.

301   Fold induction denotes activation above infected cells without antibody. Serum was obtained from 4 healthy

302   donors who had been previously vaccinated with seasonal influenza virus vaccine. Fold induction data is shown

303   as mean ± SD.

304

305   **Figure 4** Oseltamivir is more effective at preventing influenza clinical signs in animals with higher HA stalk-

306   binding antibody titers.

307

308   (A) 6-8 week old female BALB/c mice were administered 150ul of human serum or PBS i.p. and an oral gavage

309   of 0.1mg/kg of oseltamivir or PBS. The serum contains either high titers polyclonal stalk-binding antibodies

(High Serum; HS), or low titers of polyclonal stalk-binding antibodies (Low Serum; LS). The mice were then infected intranasally with 200 PFU of Viet/04 ($5 \times LD_{50}$) two hours later. Mice were given oseltamivir or PBS by oral gavage twice daily for 5 days. Weight change was monitored daily, and the animals were sacrificed when they reached 80% of initial weight.

(B-C) Weight loss and Kaplan-Meier survival curve of the Low Serum group. Weight loss is shown as percent of initial weight with mean ± SEM, n=5/group. Statistical comparisons are against the PBS Control group; *p<0.05, **p<0.01. PBS+OSLT and PBS Control groups are shared between graphs depicting High Serum and Low Serum experiments for clarity. Numbers in brackets denote number of surviving mice and total number of mice per group.

(D-E) Weight loss and Kaplan-Meier survival curve of the High Serum group. Weight loss graph is shown as percent of initial weight as mean ± SEM, n=5/group unless otherwise indicated. Statistical comparisons are against the PBS Control group; *p<0.05, **p<0.01. PBS+OSLT and PBS Control groups are shared between graphs depicting High Serum and Low Serum experiments for clarity. Numbers in brackets denote number of surviving mice and total number of mice per group.

Figure S1 Oseltamivir inhibits neuraminidase activity and replication of H1 and H3 influenza viruses.

(A-C) Neuraminidase activity of influenza viruses PR8, Cal/09, and X-31 were measured in-vitro using the NA-Star Neuraminidase Kit (ThermoFisher). Data shown as mean ± SD of at least two technical replicates.

(D-F) Oseltamivir susceptibility of the strains were then determined using 1×10^6 PFU of the three strains using the NA-Star Neuraminidase Kit (ThermoFisher). The IC_{50} values are displayed to the right of the graphs. Data shown as mean ± SD of three technical replicates.

(G-I) Oseltamivir sensitivity of influenza virus strains was also quantified using plaque assays by infecting A549 cells with the virus at an MOI of 5 before incubating the infected cells with indicated concentrations of oseltamivir for 18 hours. N.D: not detectable. The limit of detection for the plaque assays was 25 PFU/ml, denoted by the horizontal dotted line. Data shown as mean ± SD of three technical replicates.

Figure S2 Immunostaining of infected A549 cells by bNAbs.
A549 cells infected with PR8 or Cal/09 were stained with 6F12 or 6F12 D265A, and cells infected with X-31 were stained with 9H10. Uninfected A549 cells were stained using 6F12, 6F12 D265A, and 9H10 as negative controls. Scale bars = 400 μm.

345

346 **Figure S3** Characterization of polyclonal stalk-binding antibodies in human serum. Human serum was obtained

347 from peripheral blood of two healthy adult donors.

348

349 (A-B) ELISAs were performed using chimeric cH6/1 protein to quantify the titers of antibodies that bind to the

350 stalk domain of H1 hemagglutinin. Absorbance data is shown as mean ± SD with technical triplicates. The area

351 under the curve is also shown as mean ± SEM.

352

353 (C) Hemagglutinin inhibition assays using were used to test for the presence of antibodies inhibit receptor

354 binding by the head domain of Viet/04 H5. N.D. = Not detectable.

355

356 (D) In vitro ADCC assays were completed using A549 cells infected with Viet/04 (H5N1) at an MOI of 5. Fold

357 induction denotes activation above background (infected cells without antibody). Fold induction data is shown

358 as mean ± SD with technical triplicates.

359

360 **Materials and Methods (1456 words)**

361

362 **Cells and Viruses**

363 Human adenocarcinoma alveolar basal epithelial cells (A549) and Madin-Darby Canine Kidney cells (MDCK)

364 originally obtained from the ATCC were grown in "complete DMEM", containing DMEM supplemented with

365 10% (vol/vol) heat-inactivated FBS (Gibco), 100U/mL Penicillin-Streptomycin (Gibco), 2mM GlutaMAX

366 Supplement (ThermoFisher), 10mM HEPES. PR8, X-31, and Viet/04 H5N1 HAlo viruses were propagated in

367 specific pathogen free embryonated chicken eggs (Canadian Food Inspection Agency) (Kilbourne, 1969; Steel

368 et al., 2009). Cal/09 H1N1 was propagated in MDCK cells.

369

370 **NA-Star Neuraminidase Assays**

371 NA-Star assays were completed according to manufacturer's protocol (Invitrogen). Briefly, viruses were diluted

372 in NA-Star Assay Buffer in white 96 well opaque flat-bottom plates to a final volume of 25 μl per well. An

373 additional 25 μl per well of oseltamivir carboxylate (Toronto Research Chemicals) diluted in NA-Star Assay

374 Buffer was added in half-log dilutions to each well. Plates were then incubated for 20 minutes at 37 °C after

375 brief shaking. After the incubation, 10 μl of NA-Star Substrate was added to each well and was then incubated

376 for 30 minutes at room temperature after a brief shaking. After the incubation, 60 μl of NA-Star Accelerator

377 was added to each well, and luminescence was quantified using a SpectraMax i3 plate reader (Molecular

378 Devices).

379

Virus Quantification by Plaque Assay

380 MDCK cells were seeded at a density of 1×10^6 cells per well in 6 well plates. The next day, cells were infected

382 with serial dilutions of virus diluted in $1\times$ minimum essential medium (MEM, Sigma) supplemented with 0.6%

383 BSA (Sigma). After the 1-hour infection at 37°C, the media was replaced with "Flu Media" containing 1x

384 MEM, 0.6 % BSA, 1μg/ml TPCK-treated trypsin, 0.01% DEAE-dextran, and 0.5% agar. The infected cells

385 were then incubated at 37 °C for 2 days. After the incubation, the cells were fixed with 10 % buffered formalin

386 for 30 minutes at room temperature. The agar layer was then removed, and the cells were stained with crystal

387 violet to visualize plaques.

388

ADCC Reporter Assay

390 A549 cells were seeded at a density of 2×10^4 cells per well in white 96 well opaque flat-bottom plates in

391 complete DMEM. 24 hours after seeding, cells were infected with PR8, Cal/09, X-31, or Viet/04 at an MOI of

392 5. 16 hours after infection, the media was replaced with 50 μl of assay buffer (RPMI 1640 supplemented with

393 4% (vol/vol) low IgG FBS) containing oseltamivir carboxylate (Toronto Research Chemicals) and serial

394 dilutions of monoclonal antibodies or serum. After a 30-minute incubation at 37 °C, 25 μl of 7.5×10^4 Jurkat

395 effector cells expressing either human FcγRIIIa or murine FcγRIV (Promega) resuspended in assay buffer were

396 added to each well. The cells were incubated for an additional 6 hours at 37°C before 75μl of Bio-Glo

397 Luciferase Assay Reagent (Promega) was added to each well. After a 5-minute incubation at room temperature,

398 luminescence in relative light units (RLU) was quantified using a SpectraMax i3 plate reader (Molecular

399 Devices). Fold induction was obtained by dividing the RLU of the wells of interest by the mean of control wells

400 containing infected target cells and Jurkat effector cells with no monoclonal antibodies/serum.

401

Immunofluorescent Staining

403 A549 cells were seeded at a density of 2×10^4 cells per well in transparent 96 well flat-bottom plates in complete

404 DMEM. 24 hours after seeding, cells were infected with PR8, Cal/09, or X-31 at an MOI of 5. 16 hours after

405 infection, the cells were fixed using 10 % buffered formalin for 30 minutes at room temperature. After 3 washes

406 with PBS, cells were stained with 6F12, 6F12 D265A, or 9H10 at a concentration of 10 μg/ml diluted in PBS

407 for one hour. After 3 washes with PBS, the cells were then stained using 0.5 μg/ml Goat anti-mouse IgG (H+L)

408 secondary antibody Alexa Fluor 488 (Invitrogen) diluted in PBS for one hour. After 3 washes with PBS, the

409 cells were stained for 5 minutes with 1μg/ml Hoechst 33342 (Life Technologies). The cells were washed again

410 with PBS, and images were taken on an EVOS FL Cell Imaging System (ThermoFisher).

411

Antibody Purification

Murine 6F12 and 9H10 were obtained from hybridoma cultures as previously described (Tan et al., 2014, 2012). Hybridomas were thawed and expanded in ClonaCell-HY Growth Medium E (Stem Cell Technologies) up to a volume of 300ml. The media was then changed to Hybridoma-SFM (Gibco). The hybridoma cultures were harvested by centrifugation at $3000 \times g$ for 20 minutes when cultures reached maximal cell density. The supernatant was then nutated overnight at 4 °C with 1 ml of Protein G Sepharose 4 Fast Flow slurry (Invitrogen) per 25ml of supernatant. After incubation, the supernatant/Sepharose bead slurry was passed through a 5 ml polypropylene gravity flow column (Qiagen). The column was washed with 1 column volume of PBS before being eluted with 9 ml of Elution Buffer (0.1M Glycine/HCl buffer, pH 2.2) into 1 ml of Neutralization Buffer (2M Tris-HCl, pH 10). The eluate was then concentrated and buffer exchanged to PBS using 30 kDa Amicon Ultra-15 Centrifugal Filter Units (Millipore) according to the manufacturer's instructions.

The variable heavy and light chain sequences of 6F12 were cloned into the EcoRI/NheI sites of pFUSEss-CHIg-mG2a (D265A, Invivogen) and the EcoRI/BstAPI sites of pFUSE2ss-CLIg-mk (Invivogen) respectively. The Expi293 Expression System was used to produce the 6F12 D265A antibody according to the manufacturer's protocols (ThermoFisher). A 2:1 molar ratio of light to heavy chain plasmids was used to transfect Expi293F cells. Antibodies were purified from supernatant as described above.

Mouse Infections

6-8 week old female BALB/c mice (Charles River) were anesthetized with isoflurane and intranasally infected with 40 μl of PR8 (500 PFU, $5 \times LD_{50}$) or Viet/04 (200 PFU, $5 \times LD_{50}$) diluted in PBS. The mice were administered 1 mg/kg or 10 mg/kg 6F12, 150μl of undiluted serum, or 1mg/kg or 10mg/kg Mouse IgG Isotype Control (ThermoFisher) intraperitoneally either 2 hours before infection, or 48 hours post infection as described in the main text. The mice also received 1 mg/kg or 10 mg/kg oseltamivir phosphate (Toronto Research Chemicals) by oral gavage as described in the main text. Mice were monitored daily and were sacrificed if they reached endpoint, defined as 20 % reduction in initial body weight. All animal experiments were approved by the Animal Research Ethics Board at McMaster University.

ELISA

Purified soluble cH6/1 comprised of the HA head domain of A/Mallard/Sweden/81/02 H6N1 and the stalk domain of PR8 with a C-terminal T4 trimerization domain and a 6-His tag was generated using a baculovirus expression system as previously described (Pica et al., 2012). Clear flat-bottom 96-well Immulon 4 HBX plates (ThermoFisher) were coated with 50 μl of 2 μg/ml of cH6/1 diluted in ELISA coating buffer (50 mM Na_2CO_3, 50 mM $NaHCO_3$, pH 9.4) overnight at 4 °C. After the incubation, the plates were blocked for 1 hour with 100 μl of blocking buffer (5 % milk powder in PBS with 5% Tween-20 (PBS-T)). Serum serially diluted in blocking

447 buffer was then added to the wells and incubated for 2 hours at room temperature. After the incubation, the

448 plate was washed 3 times with PBS-T. Anti-human IgG (Fab specific) – peroxidase-conjugated antibody

449 (Sigma) diluted 1:5000 in blocking buffer was added to the wells and incubated for 1 hour at room temperature.

450 After 3 additional washes with PBS-T, 50μl of reconstituted SIGMAFAST OPD (Sigma) was added to each

451 well. The reaction was stopped 10 minutes later by adding 50 μl of 3M HCl to each well, and the absorbance at

452 490nm was read using a SpectraMax i3 plate reader (Molecular Devices).

453

454 **Hemagglutinin Inhibition Assay**

455 Chicken red blood cells diluted 1:1 in Alsever's solution (Canadian Food Inspection Agency) were diluted 1:10

456 in PBS and centrifuged at $300 \times g$ for 5 minutes. The supernatant was removed, and 125 μl of the red blood cell

457 (RBC) pellet was added to 25 ml of PBS to make 0.5 % chicken RBC. Serum samples were inactivated by

458 trypsin-heat-periodate treatment by first adding 10 μl of 8 mg/ml trypsin to 20 μl of serum before heating at 56

459 °C for 30 minutes. After cooling the serum to room temperature, 60 μl of 0.011M KIO_4 was added followed by

460 a 15-minute incubation at room temperature. The periodate treatment was inactivated by adding 60 μl of 1%

461 glycerol (v/v) in PBS followed by a 15-minute incubation at room temperature. Lastly, 50 μl of 0.85 % NaCl

462 (w/v) in distilled water was added to each sample to make a final 1:10 dilution of serum. The inactivated serum

463 was then diluted 1:2 across clear V-bottom plates (Sigma) to a final volume of 25 μl. Then, 4 HA units of virus

464 diluted PBS to a final volume of 25 μl was added to each well. Lastly, 50 μl of 0.5% chicken RBC was added to

465 each well. The plates were read after a 1-hour incubation at 4°C.
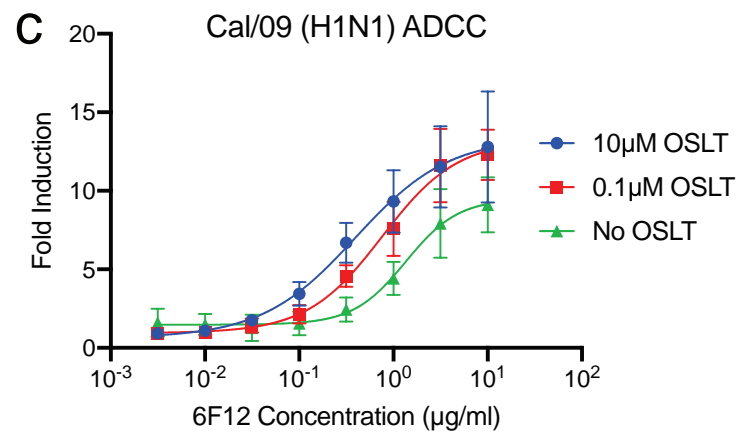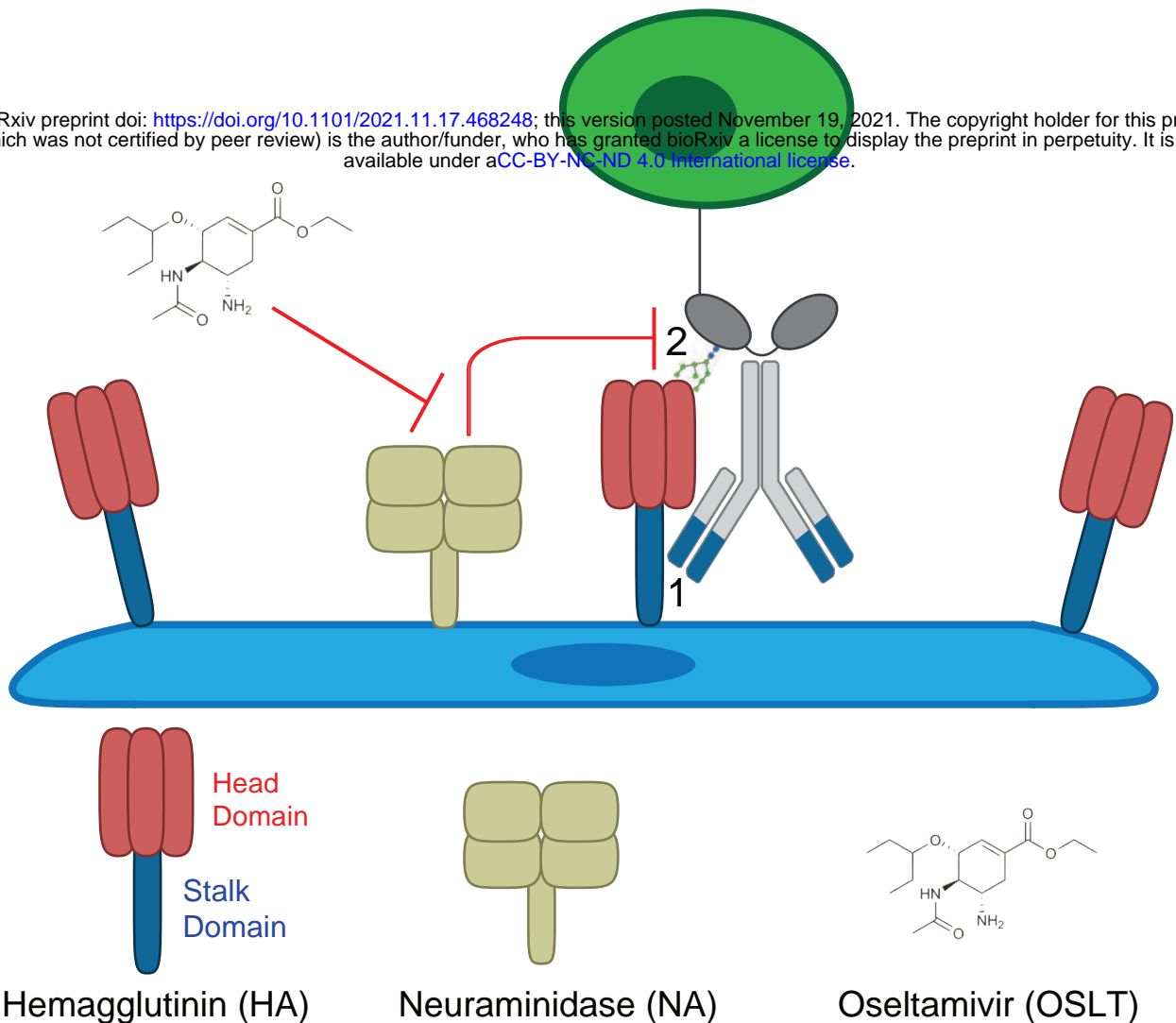
466

467 **References**

468

469 Baudino, L., Shinohara, Y., Nimmerjahn, F., Furukawa, J., Nakata, M., Martínez-Soria, E., Petry, F., Ravetch, J.V.,
470   Nishimura, S., Izui, S., 2008. Crucial role of aspartic acid at position 265 in the CH2 domain for murine
471   IgG2a and IgG2b Fc-associated effector functions. J Immunol 181, 6664–6669.
472   https://doi.org/10.4049/jimmunol.181.9.6664
473 Chromikova, V., Tan, J., Aslam, S., Rajabhathor, A., Bermudez-Gonzalez, M., Ayllon, J., Simon, V., García-Sastre,
474   A., Salaun, B., Nachbagauer, R., Krammer, F., 2020. Activity of human serum antibodies in an influenza
475   virus hemagglutinin stalk-based ADCC reporter assay correlates with activity in a CD107a degranulation
476   assay. Vaccine 38, 1953–1961. https://doi.org/10.1016/j.vaccine.2020.01.008
477 DiLillo, D.J., Palese, P., Wilson, P.C., Ravetch, J.V., 2016. Broadly neutralizing anti-influenza antibodies require Fc
478   receptor engagement for in vivo protection. J Clin Invest 126, 605–610. https://doi.org/10.1172/JCI84428
479 DiLillo, D.J., Tan, G.S., Palese, P., Ravetch, J.V., 2014. Broadly neutralizing hemagglutinin stalk-specific antibodies
480   require FcγR interactions for protection against influenza virus in vivo. Nat Med 20, 143–151.
481   https://doi.org/10.1038/nm.3443
482 Doll, M.K., Winters, N., Boikos, C., Kraicer-Melamed, H., Gore, G., Quach, C., 2017. Safety and effectiveness of
483   neuraminidase inhibitors for influenza treatment, prophylaxis, and outbreak control: a systematic review of
484   systematic reviews and/or meta-analyses. Journal of Antimicrobial Chemotherapy 72, 2990–3007.
485   https://doi.org/10.1093/jac/dkx271
486 Fry, A.M., Goswami, D., Nahar, K., Sharmin, A.T., Rahman, M., Gubareva, L., Azim, T., Bresee, J., Luby, S.P.,
487   Brooks, W.A., 2014. Efficacy of oseltamivir treatment started within 5 days of symptom onset to reduce

488 influenza illness duration and virus shedding in an urban setting in Bangladesh: a randomised placebo-
489 controlled trial. Lancet Infect Dis 14, 109–118. https://doi.org/10.1016/S1473-3099(13)70267-6
490 He, W., Chen, C.-J., Mullarkey, C.E., Hamilton, J.R., Wong, C.K., Leon, P.E., Uccellini, M.B., Chromikova, V.,
491 Henry, C., Hoffman, K.W., Lim, J.K., Wilson, P.C., Miller, M.S., Krammer, F., Palese, P., Tan, G.S., 2017.
492 Alveolar macrophages are critical for broadly-reactive antibody-mediated protection against influenza A
493 virus in mice. Nat Commun 8, 846. https://doi.org/10.1038/s41467-017-00928-3
494 He, W., Tan, G.S., Mullarkey, C.E., Lee, A.J., Lam, M.M.W., Krammer, F., Henry, C., Wilson, P.C., Ashkar, A.A.,
495 Palese, P., Miller, M.S., 2016. Epitope specificity plays a critical role in regulating antibody-dependent cell-
496 mediated cytotoxicity against influenza A virus. Proc Natl Acad Sci U S A 113, 11931–11936.
497 https://doi.org/10.1073/pnas.1609316113
498 Hiba, V., Chowers, M., Levi-Vinograd, I., Rubinovitch, B., Leibovici, L., Paul, M., 2011. Benefit of early treatment
499 with oseltamivir in hospitalized patients with documented 2009 influenza A (H1N1): retrospective cohort
500 study. J Antimicrob Chemother 66, 1150–1155. https://doi.org/10.1093/jac/dkr089
501 Iuliano, A.D., Roguski, K.M., Chang, H.H., Muscatello, D.J., Palekar, R., Tempia, S., Cohen, C., Gran, J.M.,
502 Schanzer, D., Cowling, B.J., Wu, P., Kyncl, J., Ang, L.W., Park, M., Redlberger-Fritz, M., Yu, H.,
503 Espenhain, L., Krishnan, A., Emukule, G., van Asten, L., Pereira da Silva, S., Aungkulanon, S., Buchholz,
504 U., Widdowson, M.-A., Bresee, J.S., Global Seasonal Influenza-associated Mortality Collaborator Network,
505 2018. Estimates of global seasonal influenza-associated respiratory mortality: a modelling study. Lancet 391,
506 1285–1300. https://doi.org/10.1016/S0140-6736(17)33293-2
507 Jefferson, T., Jones, M., Doshi, P., Spencer, E.A., Onakpoya, I., Heneghan, C.J., 2014. Oseltamivir for influenza in
508 adults and children: systematic review of clinical study reports and summary of regulatory comments. BMJ
509 348, g2545. https://doi.org/10.1136/bmj.g2545
510 Jegaskanda, S., Co, M.D.T., Cruz, J., Subbarao, K., Ennis, F.A., Terajima, M., 2017. Induction of H7N9-Cross-
511 Reactive Antibody-Dependent Cellular Cytotoxicity Antibodies by Human Seasonal Influenza A Viruses
512 that are Directed Toward the Nucleoprotein. J Infect Dis 215, 818–823. https://doi.org/10.1093/infdis/jiw629
513 Kilbourne, E.D., 1969. Future influenza vaccines and the use of genetic recombinants. Bull World Health Organ 41,
514 643–645.
515 Kirkpatrick, E., Qiu, X., Wilson, P.C., Bahl, J., Krammer, F., 2018. The influenza virus hemagglutinin head evolves
516 faster than the stalk domain. Sci Rep 8. https://doi.org/10.1038/s41598-018-28706-1
517 Kosik, I., Angeletti, D., Gibbs, J.S., Angel, M., Takeda, K., Kosikova, M., Nair, V., Hickman, H.D., Xie, H., Brooke,
518 C.B., Yewdell, J.W., 2019. Neuraminidase inhibition contributes to influenza A virus neutralization by anti-
519 hemagglutinin stem antibodies. J Exp Med 216, 304–316. https://doi.org/10.1084/jem.20181624
520 Lampejo, T., 2020. Influenza and antiviral resistance: an overview. Eur J Clin Microbiol Infect Dis 39, 1201–1208.
521 https://doi.org/10.1007/s10096-020-03840-9
522 Lee, Y.-N., Lee, Y.-T., Kim, M.-C., Hwang, H.S., Lee, J.S., Kim, K.-H., Kang, S.-M., 2014. Fc receptor is not
523 required for inducing antibodies but plays a critical role in conferring protection after influenza M2
524 vaccination. Immunology 143, 300–309. https://doi.org/10.1111/imm.12310
525 Leon, P.E., He, W., Mullarkey, C.E., Bailey, M.J., Miller, M.S., Krammer, F., Palese, P., Tan, G.S., 2016. Optimal
526 activation of Fc-mediated effector functions by influenza virus hemagglutinin antibodies requires two points
527 of contact. Proc Natl Acad Sci U S A 113, E5944–E5951. https://doi.org/10.1073/pnas.1613225113
528 Miller, M.S., Gardner, T.J., Krammer, F., Aguado, L.C., Tortorella, D., Basler, C.F., Palese, P., 2013a. Neutralizing
529 antibodies against previously encountered influenza virus strains increase over time: a longitudinal analysis.
530 Sci Transl Med 5, 198ra107. https://doi.org/10.1126/scitranslmed.3006637
531 Miller, M.S., Palese, P., 2014. Peering into the crystal ball: influenza pandemics and vaccine efficacy. Cell 157,
532 294–299. https://doi.org/10.1016/j.cell.2014.03.023
533 Miller, M.S., Tsibane, T., Krammer, F., Hai, R., Rahmat, S., Basler, C.F., Palese, P., 2013b. 1976 and 2009 H1N1
534 Influenza Virus Vaccines Boost Anti-Hemagglutinin Stalk Antibodies in Humans. The Journal of Infectious
535 Diseases 207, 98–105. https://doi.org/10.1093/infdis/jis652
536 Nachbagauer, R., Choi, A., Izikson, R., Cox, M.M., Palese, P., Krammer, F., 2016. Age Dependence and Isotype
537 Specificity of Influenza Virus Hemagglutinin Stalk-Reactive Antibodies in Humans. mBio 7, e01996-01915.
538 https://doi.org/10.1128/mBio.01996-15
539 Nachbagauer, R., Wohlbold, T.J., Hirsh, A., Hai, R., Sjursen, H., Palese, P., Cox, R.J., Krammer, F., 2014. Induction
540 of Broadly Reactive Anti-Hemagglutinin Stalk Antibodies by an H5N1 Vaccine in Humans. Journal of
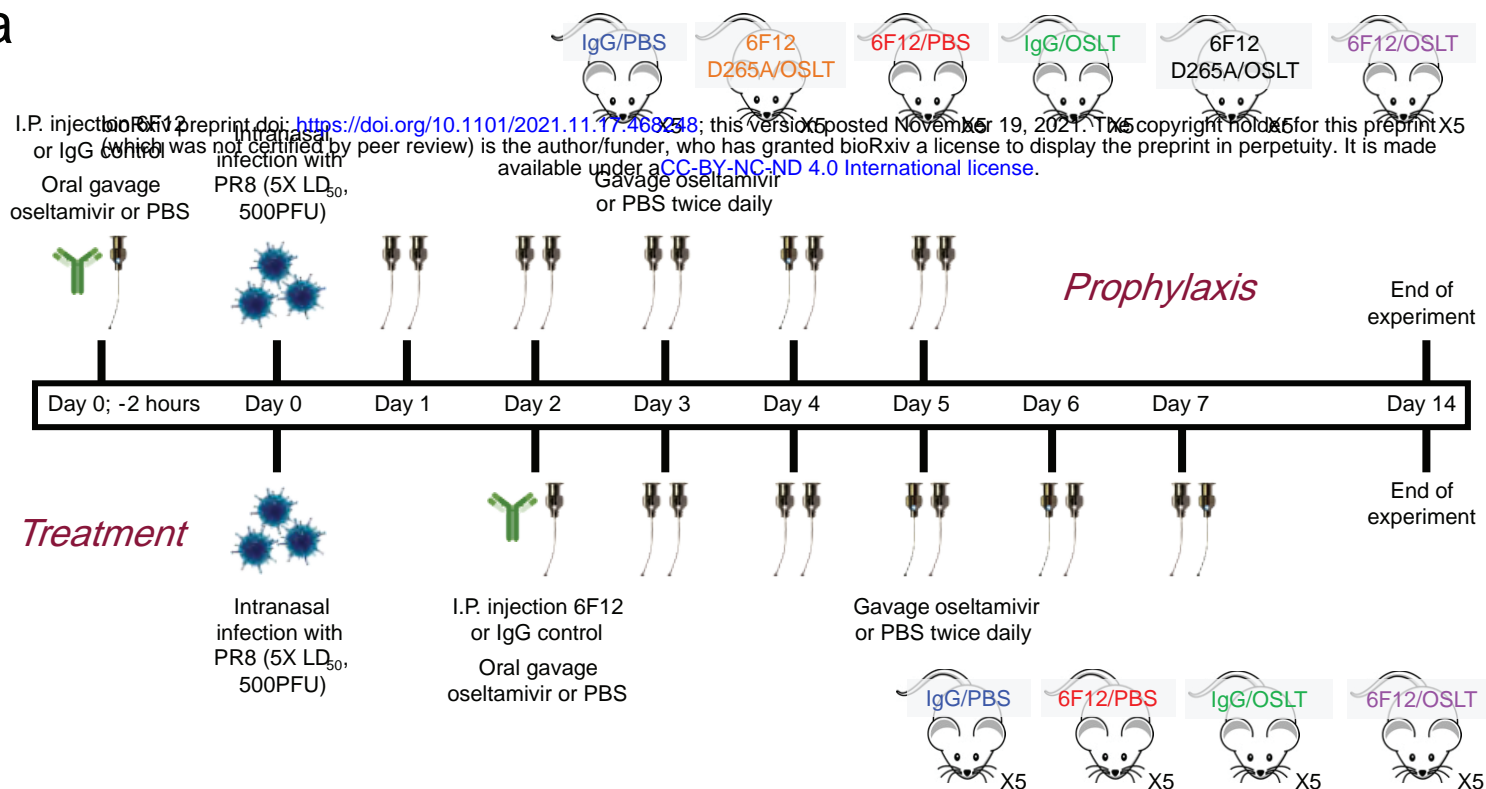541 Virology 88, 13260. https://doi.org/10.1128/JVI.02133-14

Nakamura, G., Chai, N., Park, S., Chiang, N., Lin, Z., Chiu, H., Fong, R., Yan, D., Kim, J., Zhang, J., Lee, W.P., Estevez, A., Coons, M., Xu, M., Lupardus, P., Balazs, M., Swem, L.R., 2013. An in vivo human-plasmablast enrichment technique allows rapid identification of therapeutic influenza A antibodies. Cell Host Microbe 14, 93–103. https://doi.org/10.1016/j.chom.2013.06.004

Nimmerjahn, F., Bruhns, P., Horiuchi, K., Ravetch, J.V., 2005. FcgammaRIV: a novel FcR with distinct IgG subclass specificity. Immunity 23, 41–51. https://doi.org/10.1016/j.immuni.2005.05.010

Noshi, T., Kitano, M., Taniguchi, K., Yamamoto, A., Omoto, S., Baba, K., Hashimoto, T., Ishida, K., Kushima, Y., Hattori, K., Kawai, M., Yoshida, R., Kobayashi, M., Yoshinaga, T., Sato, A., Okamatsu, M., Sakoda, Y., Kida, H., Shishido, T., Naito, A., 2018. In vitro characterization of baloxavir acid, a first-in-class cap-dependent endonuclease inhibitor of the influenza virus polymerase PA subunit. Antiviral Research 160, 109–117. https://doi.org/10.1016/j.antiviral.2018.10.008

Paules, C.I., Lakdawala, S., McAuliffe, J.M., Paskel, M., Vogel, L., Kallewaard, N.L., Zhu, Q., Subbarao, K., 2017. The Hemagglutinin A Stem Antibody MEDI8852 Prevents and Controls Disease and Limits Transmission of Pandemic Influenza Viruses. J Infect Dis 216, 356–365. https://doi.org/10.1093/infdis/jix292

Pica, N., Hai, R., Krammer, F., Wang, T.T., Maamary, J., Eggink, D., Tan, G.S., Krause, J.C., Moran, T., Stein, C.R., Banach, D., Wrammert, J., Belshe, R.B., García-Sastre, A., Palese, P., 2012. Hemagglutinin stalk antibodies elicited by the 2009 pandemic influenza virus as a mechanism for the extinction of seasonal H1N1 viruses. Proc Natl Acad Sci U S A 109, 2573–2578. https://doi.org/10.1073/pnas.1200039109

Rodríguez, A., Díaz, E., Martín-Loeches, I., Sandiumenge, A., Canadell, L., Díaz, J.J., Figueira, J.C., Marques, A., Alvarez-Lerma, F., Vallés, J., Baladín, B., García-López, F., Suberviola, B., Zaragoza, R., Trefler, S., Bonastre, J., Blanquer, J., Rello, J., H1N1 SEMICYUC Working Group, 2011. Impact of early oseltamivir treatment on outcome in critically ill patients with 2009 pandemic influenza A. J Antimicrob Chemother 66, 1140–1149. https://doi.org/10.1093/jac/dkq511

Sangster, M.Y., Baer, J., Santiago, F.W., Fitzgerald, T., Ilyushina, N.A., Sundararajan, A., Henn, A.D., Krammer, F., Yang, H., Luke, C.J., Zand, M.S., Wright, P.F., Treanor, J.J., Topham, D.J., Subbarao, K., 2013. B Cell Response and Hemagglutinin Stalk-Reactive Antibody Production in Different Age Cohorts following 2009 H1N1 Influenza Virus Vaccination. Clinical and Vaccine Immunology : CVI 20, 867. https://doi.org/10.1128/CVI.00735-12

Stacey, H.D., Golubeva, D., Posca, A., Ang, J.C., Novakowski, K.E., Zahoor, M.A., Kaushic, C., Cairns, E., Bowdish, D.M.E., Mullarkey, C.E., Miller, M.S., 2021. IgA Potentiates NETosis in Response to Viral Infection. bioRxiv 2021.01.04.424830. https://doi.org/10.1101/2021.01.04.424830

Stadlbauer, D., Zhu, X., McMahon, M., Turner, J.S., Wohlbold, T.J., Schmitz, A.J., Strohmeier, S., Yu, W., Nachbagauer, R., Mudd, P.A., Wilson, I.A., Ellebedy, A.H., Krammer, F., 2019. Broadly protective human antibodies that target the active site of influenza virus neuraminidase. Science 366, 499–504. https://doi.org/10.1126/science.aay0678

Steel, J., Lowen, A.C., Pena, L., Angel, M., Solórzano, A., Albrecht, R., Perez, D.R., García-Sastre, A., Palese, P., 2009. Live attenuated influenza viruses containing NS1 truncations as vaccine candidates against H5N1 highly pathogenic avian influenza. J Virol 83, 1742–1753. https://doi.org/10.1128/JVI.01920-08

Tan, G.S., Krammer, F., Eggink, D., Kongchanagul, A., Moran, T.M., Palese, P., 2012. A pan-H1 anti-hemagglutinin monoclonal antibody with potent broad-spectrum efficacy in vivo. J Virol 86, 6179–6188. https://doi.org/10.1128/JVI.00469-12

Tan, G.S., Lee, P.S., Hoffman, R.M.B., Mazel-Sanchez, B., Krammer, F., Leon, P.E., Ward, A.B., Wilson, I.A., Palese, P., 2014. Characterization of a broadly neutralizing monoclonal antibody that targets the fusion domain of group 2 influenza A virus hemagglutinin. J Virol 88, 13580–13592. https://doi.org/10.1128/JVI.02289-14

Temming, A.R., Bentlage, A.E.H., de Taeye, S.W., Bosman, G.P., Lissenberg-Thunnissen, S.N., Derksen, N.I.L., Brasser, G., Mok, J.Y., van Esch, W.J.E., Howie, H.L., Zimring, J.C., Vidarsson, G., 2020. Cross-reactivity of mouse IgG subclasses to human Fc gamma receptors: Antibody deglycosylation only eliminates IgG2b binding. Mol Immunol 127, 79–86. https://doi.org/10.1016/j.molimm.2020.08.015

Wu, N.C., Wilson, I.A., 2017. A perspective on the structural and functional constraints for immune evasion: insights from the influenza virus. J Mol Biol 429, 2694–2709. https://doi.org/10.1016/j.jmb.2017.06.015
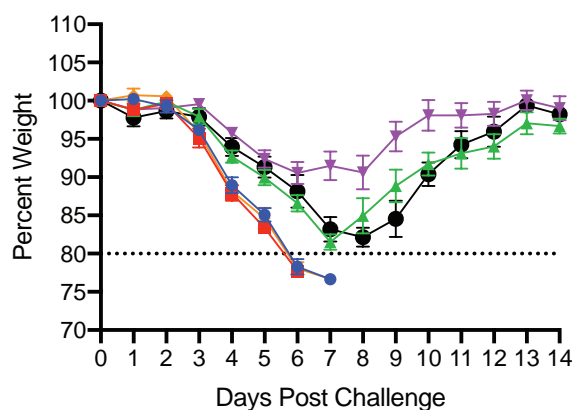
a. cH6/1 ELISA — Absorbance (490nm) vs Reciprocal Serum Dilution for Donor 1, Donor 2, Donor 3, Donor 4

b. cH6/1 ELISA — Area Under the Curve for Donor 1, Donor 2, Donor 3, Donor 4
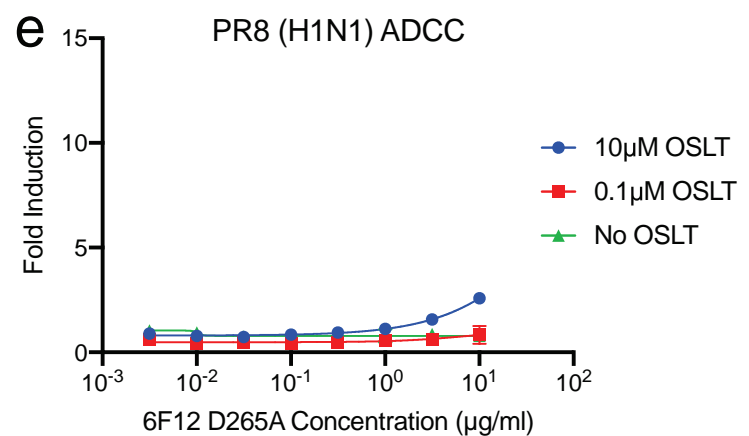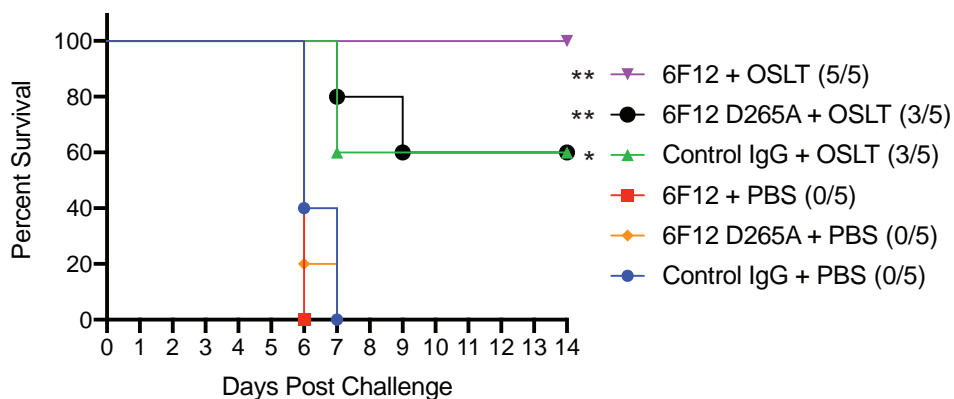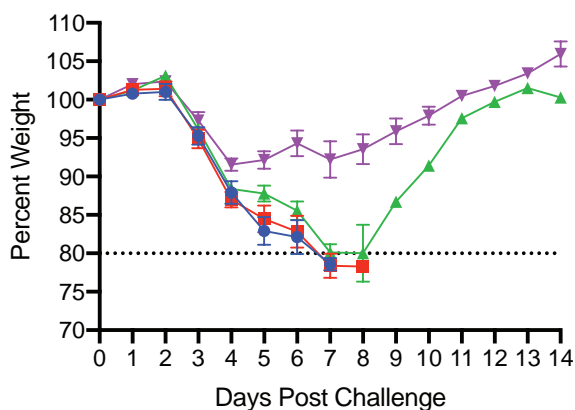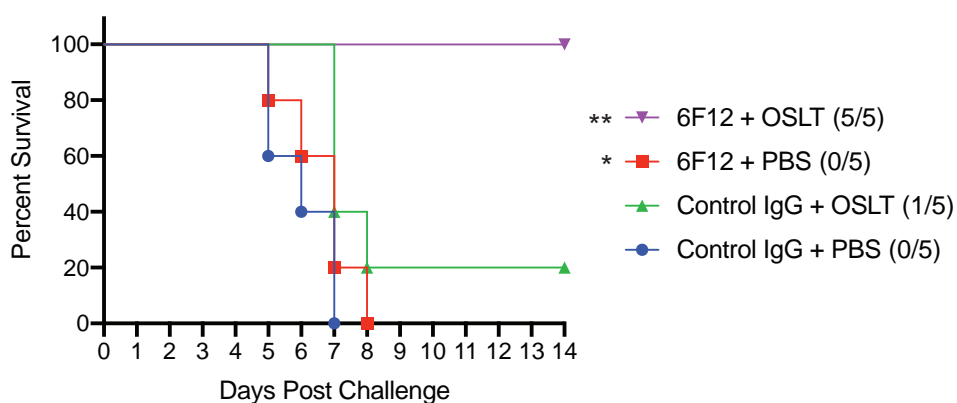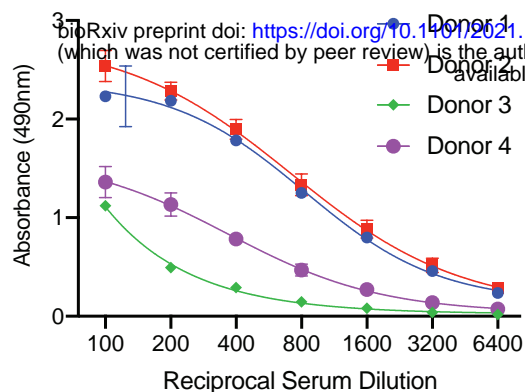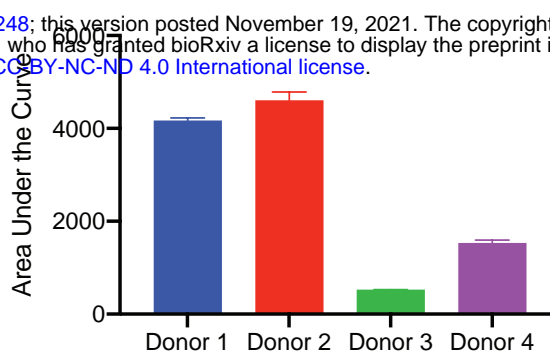
c. Donor 1 Viet/04 (H5N1) ADCC — Fold Induction vs Reciprocal Serum Dilution; Serum + 10µM OSLT, Serum Alone
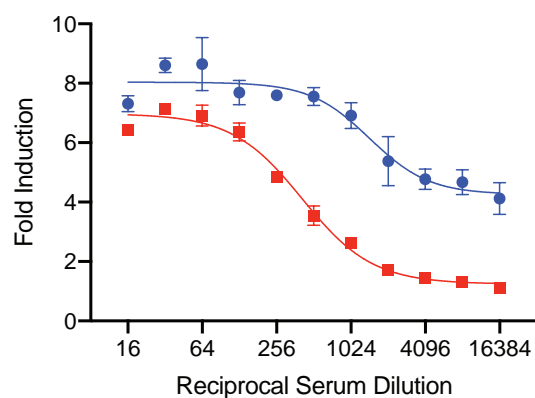
d. Donor 2 Viet/04 (H5N1) ADCC — Fold Induction vs Reciprocal Serum Dilution; Serum + 10µM OSLT, Serum Alone
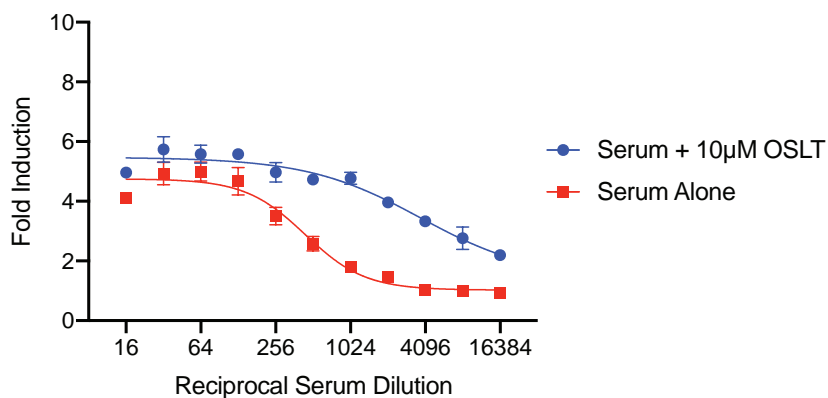
e. Donor 3 Viet/04 (H5N1) ADCC — Fold Induction vs Reciprocal Serum Dilution; Serum + 10µM OSLT, Serum Alone
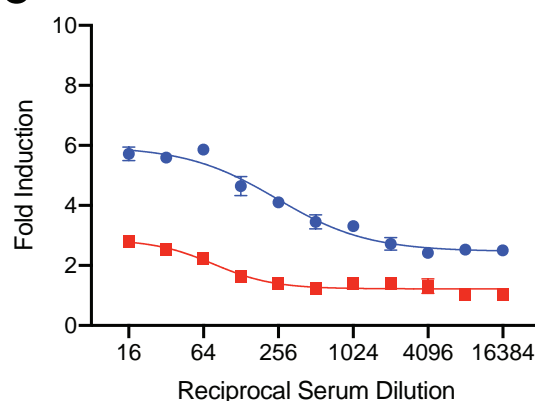
f. Donor 4 Viet/04 (H5N1) ADCC — Fold Induction vs Reciprocal Serum Dilution; Serum + 10µM OSLT, Serum Alone

a

PBS/PBS   LS/PBS   HS/PBS   PBS/OSLT   S/OSLT   HS/OSLT

Prophylaxis

X5   X5   X5   X5   X5   X5

End of experiment

| Day 0; -2 hours | Day 0 | Day 1 | Day 2 | Day 3 | Day 4 | Day 5 | Day 14 |

End of experiment

Intranasal infection with PR8 (5X LD$_{50}$, 500PFU)

Gavage oseltamivir or PBS twice daily
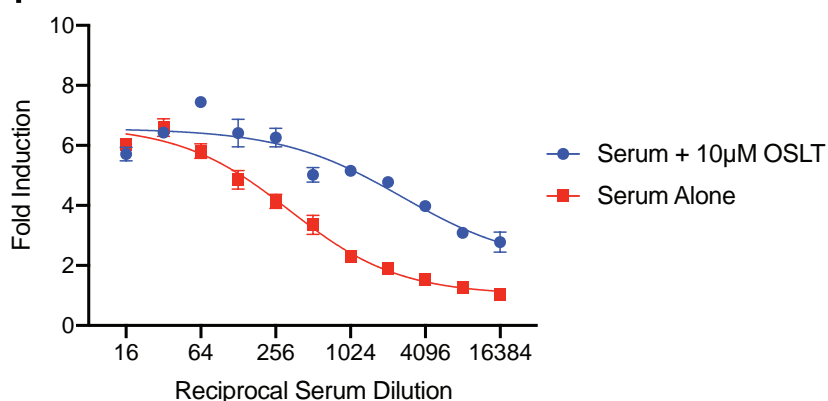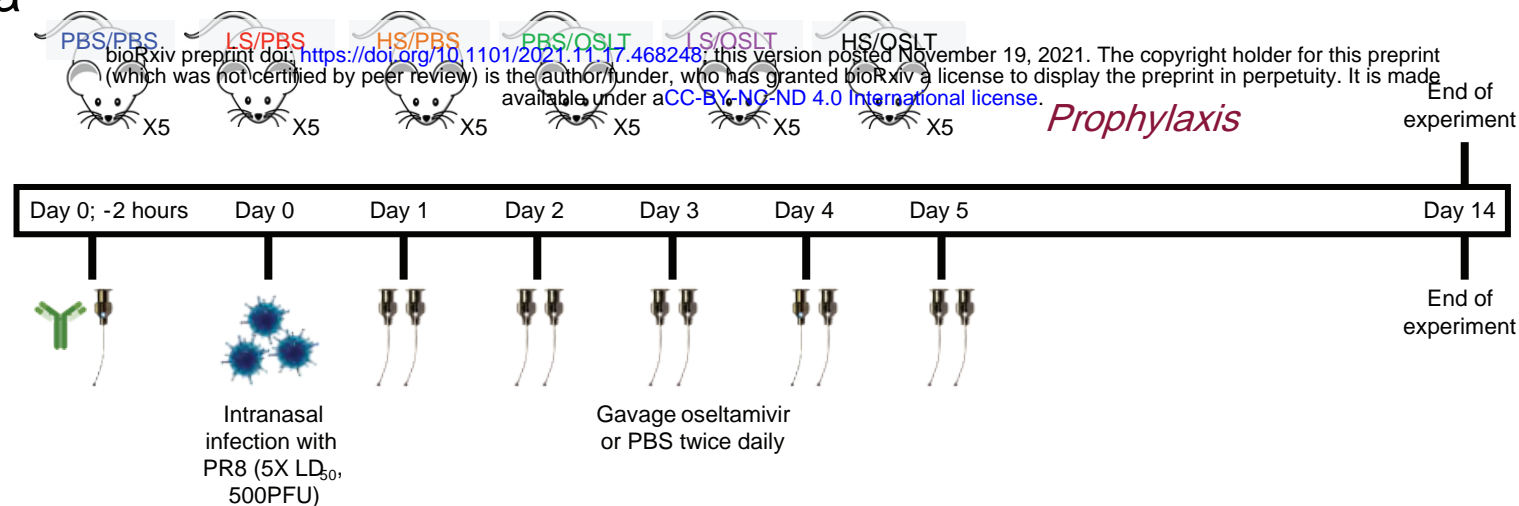
b Viet/04 (5×LD$_{50}$) Low Serum Prophylaxis

c Viet/04 (5×LD$_{50}$) Low Serum Prophylaxis

** Low Serum + OSLT (4/5)
** PBS + OSLT (1/5)
** Low Serum + PBS (1/5)
PBS Control (0/5)
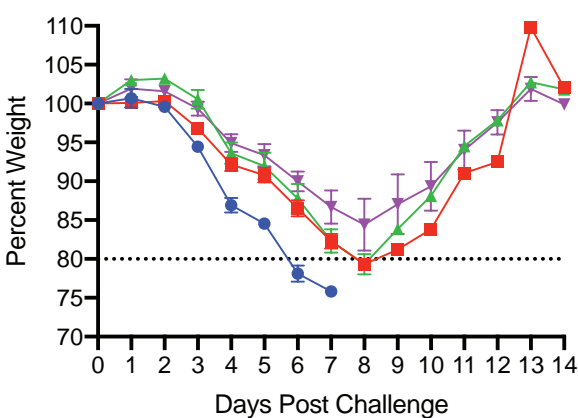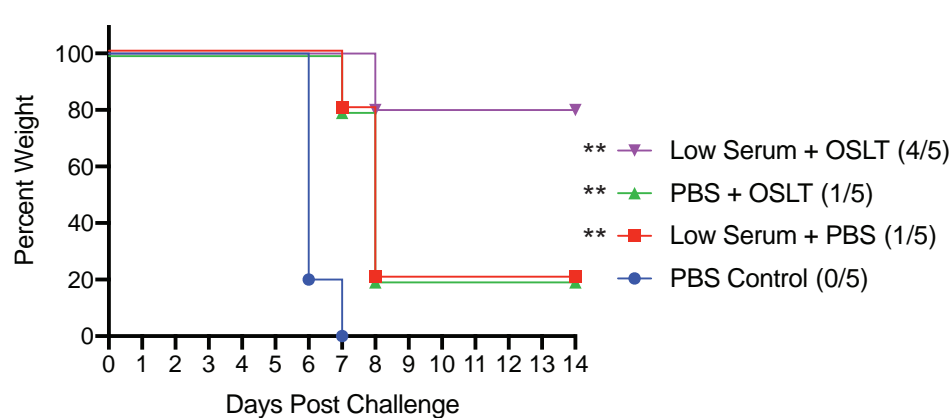
d Viet/04 (5×LD$_{50}$) High Serum Prophylaxis

e Viet/04 (5×LD$_{50}$) High Serum Prophylaxis

** High Serum + OSLT (5/5)
** PBS + OSLT (1/5)
High Serum + PBS (0/4)
PBS Control (0/5)